Acta Oceanol. Sin., 2024, Vol. 43, No. 8, P. 47–57
https://doi.org/10.1007/s13131-024-2292-0
http://www.aosocean.com
E-mail: ocean2@hyxb.org.cn

Diatoms as indicators of environmental change in coastal areas: a case study in Lianjiang coast of East China Sea

Tong Li[1, 2], Jihui Zhang[2], Dongling Li[1, 2*], Chengxu Zhou[3], Chenxi Liu[1, 2], Hao Xu[1, 2], Bing Song[4], Longbin Sha[1, 2]

[1] Donghai Academy, Ningbo University, Ningbo 315211, China

[2] Department of Geography and Spatial Information Techniques, Ningbo University, Ningbo 315211, China

[3] College of Food Science and Engineering, Ningbo University, Ningbo 315211, China

[4] State Key Laboratory of Lake Science and Environment, Nanjing Institute of Geography and Limnology, Chinese Academy of Sciences, Nanjing 210008, China

Received 26 September 2023; accepted 24 December 2023

Abstract

Owing to the significant differences in environmental characteristics and explanatory factors among estuarine and coastal regions, research on diatom transfer functions and database establishment remains incomplete. This study analysed diatoms in surface sediment samples and a sediment core from the Lianjiang coast of the East China Sea, together with environmental variables. Principal component analysis of the environmental variables showed that sea surface salinity (SSS) and sea surface temperature were the most important factors controlling hydrological conditions in the Lianjiang coastal area, whereas canonical correspondence analysis indicated that SSS and pH were the main environmental factors affecting diatom distribution. Based on the modern diatom species–environmental variable database, we developed a diatom-based SSS transfer function to quantitatively reconstruct the variability in SSS between 1984 and 2021 for sediment core HK3 from the Lianjiang coastal area. The agreement between the reconstructed SSS and instrument SSS data from 1984 to 2021 suggests that diatom-based SSS reconstruction is reliable for studying past SSS variability in the Lianjiang coastal area. Three low SSS events in AD 2019, 2013, and 1999, together with an increased relative concentration of freshwater diatom species and coarser sediment grain sizes, corresponded to two super-typhoon events and a catastrophic flooding event in Lianjiang County. Thus, a diatom-based SSS transfer function for reconstructing past SSS variability in the estuarine and coastal areas of the East China Sea can be further used to reflect the paleoenvironmental events in this region.

Key words: diatom, transfer function, multivariate statistical analysis, environmental variable, sea surface salinity

Citation: Li Tong, Zhang Jihui, Li Dongling, Zhou Chengxu, Liu Chenxi, Xu Hao, Song Bing, Sha Longbin. 2024. Diatoms as indicators of environmental change in coastal areas: a case study in Lianjiang coast of East China Sea. Acta Oceanologica Sinica, 43(8): 47–57, doi: 10.1007/s13131-024-2292-0

1 Introduction

Coastal estuarine areas are among the most dynamic and complex environments on Earth (Rovira et al., 2012). They function as transition zones among marine, river, and terrestrial environments and exhibit large spatiotemporal environmental gradients (Azhikodan and Yokoyama, 2015; Nwe et al., 2021). Coastal sediments have long been recognised as reliable records of marine environmental conditions (López-Belzunce et al., 2020; Triantaphyllou et al., 2009), sea-level changes (Wang et al., 2013; Yu et al., 2023a), freshwater inputs (Espinosa et al., 2022; Fayó et al., 2018), and extreme weather events (Benito et al., 2015; Nakanishi et al., 2022). Variations in freshwater input from rivers and extreme events such as storm surges can strongly disturb the water environment in coastal areas. These disturbances can be partially recorded in the physical and chemical indicators of sediments as well as in microfossil assemblages. For example, Fayó et al. (2018) used the alluvial sediments of the delta of the Colorado River to identify the historic changes in floodplain hydrology. Nakanishi et al. (2022) used diatoms and chemical analyses to reveal the history of extreme wave events in the coastal wetlands of central Hidaka. The Lianjiang coast is located on the western side of the East China Sea and is a typical coastal area with thick sediment accumulations that record river flow dynamics, ocean currents, and extreme events (Huh and Su, 1999). Thus, this area is critical for reconstructing the evolution of the coastal environment and climate.

Coastal and estuarine areas are highly productive regions, with phytoplankton being the primary producer in the food web (Nwe et al., 2021; Saifullah et al., 2019). Diatoms, one of the most important phytoplankton groups, can survive under conditions of high turbidity (Lionard et al., 2008; Mendes et al., 2009). Among the biological proxies preserved in sediments, diatoms are valuable indicators for tracing environmental changes on various timescales (Espinosa et al., 2022). They can tolerate and adapt to a wide range of environmental conditions and respond rapidly to physical, chemical, and biological variations in aquatic ecosystems; moreover, their siliceous frustules are well-preserved in sediments and have a well-defined taxonomy (Chen

Foundation item: The National Natural Science Foundation of China under contract Nos 42376236 and 42176226.
*Corresponding author, E-mail: lidongling@nbu.edu.cn

et al., 2020a; Espinosa et al., 2022; Gregersen et al., 2023). After death, planktonic and benthic diatoms sink to the sediment surface and mix with *in situ* and displaced species (Chen et al., 2019). This process reflects the local environmental conditions and provides insights into the dynamics of runoff inputs and ocean currents. Therefore, identifying the ecological variables that regulate the seasonal and interannual succession of diatom communities is valuable for monitoring and evaluating regional environmental changes (Mendes et al., 2009).

Statistical inference models based on modern species–environment relationships effectively utilise ecological data derived from biological assemblages, enabling the quantitative estimation of critical environmental parameters (Hassan et al., 2009). Thus, transfer functions are reliable for generating high-resolution quantitative estimates of paleoenvironmental conditions (Hassan et al., 2009). Over the past decades, numerous diatom-based transfer functions have been developed to infer a wide range of environmental variables in lake and marine systems. Fruitful results have been obtained in the study of the relationship between diatoms and environmental variables in freshwater ecosystems, such as temperature (Wang et al., 2014; Szczerba et al., 2023), water depth (Chen et al., 2020b), and eutrophication (Yang et al., 2008; Chen et al., 2022; Wang et al., 2012). Diatom-based environmental transfer function datasets have been established in different regions, such as Europe (Bennion et al., 2001), Asia (Yu et al., 2023b), and South America (Gomes et al., 2014). The study of marine diatom transfer functions has also made significant progress in the reconstruction of the sea level (Zong and Horton, 1999), sea surface temperature (De Sève, 1999; Li et al., 2017), and sea ice extent (Sha et al., 2015). Although the marine system includes estuarine and coastal parts, the environmental characteristics of the land-sea interface area are more distinctive than those of marine and lakes, involving a wider range of environmental factors, which make the development of transfer functions more challenging (Hassan et al., 2009). Some research has been conducted in estuaries and coastal areas. For example, Horton et al. (2006) developed the first diatom-based transfer function for the east coast of North America and used it to reconstruct sea level changes. Hassan et al. (2009) built a two-component Weighted Average (WA) Partial Least Squares (PLS) calibration model to infer salinity in three estuaries along the northeastern coast of Argentina. However, owing to the significant differences in environmental characteristics and explanatory factors among different estuarine and coastal regions, research on diatom transfer functions and database establishment remains incomplete in the East China Sea.

The objectives of this study were to (1) identify the major environmental variables affecting diatom assemblages in the Lianjiang coastal area of the East China Sea, (2) establish estuarine and coastal diatom-based transfer functions, and (3) test the reliability of the transfer functions by reconstructing past environmental events from a sediment core. Our results provide new ecological information on the relationships between diatoms and environmental parameters and their spatiotemporal distribution characteristics, which may contribute to a better understanding of estuarine and coastal ecosystems affected by rivers.

2 Materials and methods

2.1 *Environmental setting of the Lianjiang coast*

The study area is located on the eastern coast of Lianjiang County, Fujian Province, Southeast China (26.15°–26.30°N, 119.60°–119.80°E) (Fig. 1). This area has a typical mid-subtropical maritime monsoon climate with warm, humid weather and abundant rainfall (Lin et al., 2020; Peng et al., 2021). The average annual rainfall is 1 551 mm, with the wet season (March to September) receiving approximately 80% of the precipitation and the dry season (October to February) receiving the remaining approximately 20%. Typhoons are the primary weather hazards in this region. Lianjiang County experiences an average of 5.5–5.7 tropical cyclones per year (Peng et al., 2021).

Both the Aojiang River and Minjiang River entered the study area from the west (Fig. 1b). The Aojiang River is a medium-sized river, 137 km long, with a watershed area of 2 655 km^2, and an annual freshwater discharge of 2.728 × 10^9 m^3 (Lei et al., 2021; Zhang, 2014). The Minjiang River is the largest river in Fujian

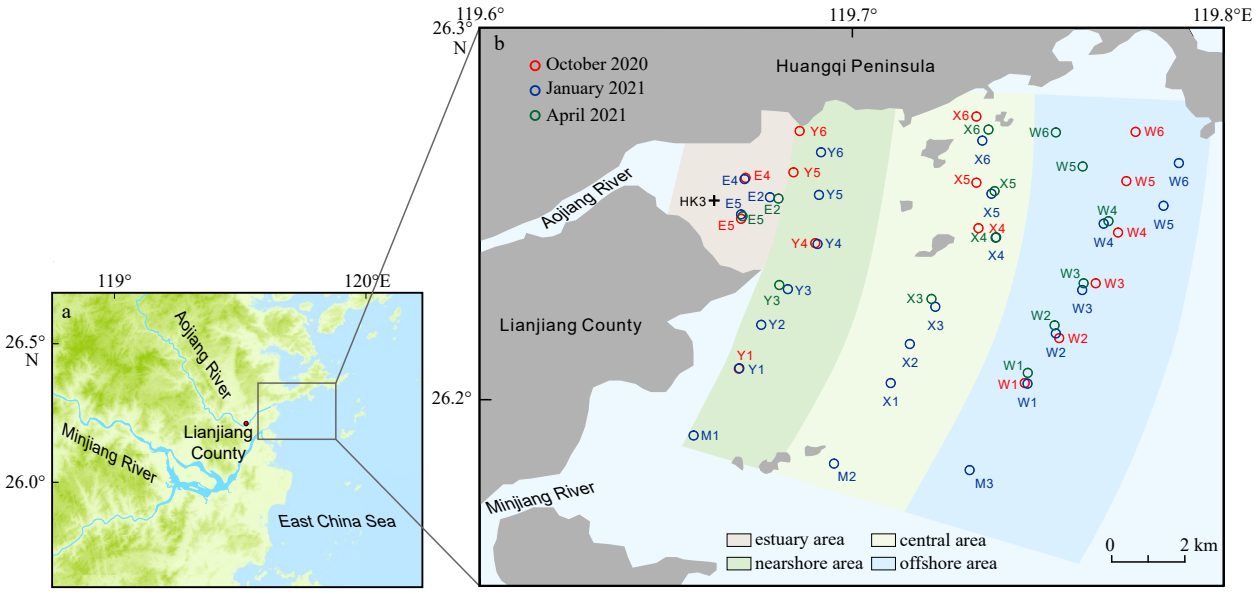

Fig. 1. Location of the study area in Lianjiang County. a. Topography and distribution of rivers in the study area. The Aojiang River is in the northern part of the figure and the Minjiang River is in the southern part; the Lianjiang coast is influenced by both rivers. b. Locations of surface sediment samples and a sediment core HK3.

Province and flows into the southern part of the study area. It is 577 km long with a drainage area of 60 992 km^2 and an average annual freshwater discharge of 6.20×10^{10} m^3 (Fan et al., 2021). Both the Aojiang River and Minjiang River have strongly tidal estuaries and are characterized by a regular semi-daily tidal range of 0.74 m to 4.5 m, with an average of 3.8 m (Peng et al., 2021).

The study area is controlled by the Zhe-Min Coastal Current; it supplies abundant nutrients to the coastal bays of Fujian in winter, together with the nutrient input maximum from the Aojiang River and Minjiang River, which have a large impact on the local aquatic environment (Xu et al., 2020). Lianjiang County was the second most important county in China for fish and shellfish products over the last three decades (Lei et al., 2021; Yang et al., 2022). The main fish species cultured were *Larimichthys crocea*, *Pagrosomus major*, *Sciaenops ocellatus*, and *Lateolabrax japonicus*. The main cultured shellfish are *Ruditapes philippinarum* on sandy beaches and *Sinonovacula constricta* on clay beaches, which are seeded in March and harvested in September (Lei et al., 2021; Zhou et al., 2022).

2.2 *Sample collection*

A total of 52 surface sediment samples were collected from the Lianjiang coast in October 2020, January 2021, and April 2021. The sampling locations are shown in Fig. 1b. The environmental parameters of each seawater sample, including sea surface temperature (SST), sea surface salinity (SSS), pH, redox potential, electrical conductivity, dissolved oxygen, total dissolved solids, and turbidity were measured using an *in situ* multiparameter water quality instrument (HORIBA U52G, Japan) at the time of sample collection (Table S1). The depths of the 52 sampling sites ranged from 1.5 m to 17 m, with an average depth of 8 m.

Sediment core HK3 was collected in October 2021 from the tidal flats of the study area (26.25°N, 119.66°E) using a mudflat sampler. The core measured 100 cm in length. Twenty samples were extracted at 5 cm intervals from the core HK3.

2.3 *Laboratory measurements*

Diatom analysis was conducted on 15–16 mg of dried sediment per sample following the preparation methods described by Håkansson (1984). Diatoms were counted and identified using a Motic BA410E microscope at 1 000× magnification. Diatoms were identified at the species or species group level following the standard taxonomic literature for marine diatoms (Guo and Qian, 2003; Jin et al., 1982; Krammer and Lange-Bertalot, 1986, 1988, 1991a, 1991b). At least 200 diatom valves were counted in random transects of most of the samples.

Diatom fluxes were calculated using the following equation (Battarbee et al., 2001):

$$A = \frac{N \times S}{n \times a \times m}, \tag{1}$$

where A is the diatom concentration (valves/g), N is the number of diatoms counted, S is the area of the Petri dish, n is the number of fields of vision counted, a is the area of one field of vision, and m is the dry weight of the sample (g).

The Shannon-Weaver diversity index (SW index) was used to reflect the biodiversity of diatoms in the samples, and the formula is as follows (Shannon and Weaver, 1949):

$$H' = -\sum_{i=1}^{S}\left(\frac{N_i}{N}\right)\log_2\left(\frac{N_i}{N}\right), \tag{2}$$

where H' is the SW index, S is the number of diatom species identified, N_i is the number of the i^{th} diatom species, and N is the total number of diatoms identified.

Grain size determination was performed on 72 samples (52 surface samples and 20 core samples) using a Beckman Coulter laser diffraction particle size analyser (LS13320, USA) with a measurement range of 0.04–2 000 μm. Samples were firstly thoroughly mixed and dried at 40℃ for 24 h and then a subsample of about 0.2 g was taken from each sample. This was followed by the addition of 5 mL HCl (10%) to eliminate carbonates, 5 mL H_2O_2 (10%) to remove organic matter, and 5 mL $(NaPO_3)_6$ to promote dispersion before testing (Jiang et al., 2020).

2.4 *Age model of core HK3*

The chronological framework of core HK3 was established by ^{210}Pb dating. After drying at low temperatures, the samples were disaggregated using a mortar and pestle to produce a uniform grain size. The activity of $^{210}Pb_{ex}$ at each level was measured using a high-purity Ge Gamma Spectrometer (GWL-120-15, USA) at the Nanjing Institute of Geography and Limnology, Chinese Academy of Sciences. To provide the best possible new insights into the sedimentary processes of the Lianjiang coast sediment accumulation from the decay-corrected $^{210}Pb_{ex}$ profiles, cores were processed using the clay-normalisation procedure. Initial $^{210}Pb_{ex}$ was recalculated by normalising to average clay based on the percent of the clay-sized sediments (<4 μm) at each sample (Sun et al., 2017, 2020).

The sediment accumulation rates were calculated using the constant initial concentration (CIC) model (Sanchez-Cabeza and Ruiz-Fernández, 2012):

$$[^{210}Pb_{(m)}] = [^{210}Pb_{(0)}]e^{-\lambda t}, \tag{3}$$

where $[^{210}Pb_{(m)}]$ is the specific activity of $[^{210}Pb_{ex}]$ (Bq/kg) at depth m, $[^{210}Pb_{(0)}]$ is the surface sediment specific activity (Bq/kg), and λ is the decay constant of $[^{210}Pb]$ (0.031 14 a^{-1}).

2.5 *Multivariate statistical analysis*

Diatom assemblages and their relationships with environmental variables were examined using multivariate statistical analysis to determine the principal variables and detect similarities among the diatom samples (Chen et al., 2016).

Principal component analysis (PCA) has the advantage of weight determination because it classifies the original data into several comprehensive variables with characterisation significance using correlation coefficients to accurately reflect the core information for the evaluation indicators (Abdi and Williams, 2010).

Canonical correspondence analysis (CCA) extracts the best synthetic gradients from data on biological communities and environmental variables and intuitively shows the characteristics of the relationship between these variables and biological taxa (Klami et al., 2013). To determine the distribution of the surface sedimentary diatom species, a detrended correspondence analysis (DCA) was required to determine the gradient length of the ordination axes before selecting the appropriate model (Chen et al., 2016). To identify the primary environmental factors influencing the distribution of surface sediment diatoms in the study area, sites with fewer than 200 diatoms were eliminated.

PCA and CCA were conducted using the CANOCO (version 5) software (Ter Braak and Smilauer, 2012). The transfer function was calculated using the C2 software developed by Juggins

(2007). The derivation ability of the model was evaluated according to the root-mean-square error of prediction ($RMSEP_{Jack}$) and squared correlation (R^2_{Jack}).

2.6 *Modern SSS data*

The modern SSS data used in this study were obtained from the World Meteorological Organization climate explorer open dataset (http://climexp.knmi.nl/start.cgi), which was averaged month by month from 1900 to 2018. Monthly gridded SSS data for 1984–2018 were selected and converted to annual data for comparison with the diatom-based SSS reconstruction of core HK3.

3 Results and discussion

3.1 *Establishing a diatom–environmental variables dataset*

3.1.1 *Diatom concentration and diversity in the surface samples*

A total of 92 diatom species belonging to 36 genera were identified in surface sediment samples from the Lianjiang coastal area. The dominant species are: *Actinocyclus kuetzingii, Actinocyclus octonarius, Amphora coffeaeformis, Cyclotella striata, Paralia sulcata, Planothidium delicatulum, Pleurosigma angulatum, Surirella armoricana, Thalassionema nitzschioides, Thalassiosira leptopus,* and *Trybliptychus cocconeisformis* (Fig. S1). Among them, *Planothidium delicatulum* and *Aulacoseira granulata* are freshwater diatoms (Hartley et al., 1996; Hustedt, 1985); *Actinocyclus octonarius*, *Cyclotella striata*, *S. armoricana*, and *Paralia sulcata* are commonly found in brackish water in estuarine areas (Jiang et al., 2004; Prelle et al., 2019; Ran and Jiang, 2005). Some marine diatom species, such as *Thalassionema nitzschioides*, exhibit strong tolerance to SST and SSS (Jousé et al., 1971).

Surface diatom concentrations and SW index values are shown in Fig. 2. In October 2020, diatom concentrations were relatively high in the estuary and offshore areas, with the highest value at site W3 in the offshore area (1.65×10^6 valves/g), followed by site E4 (1.52×10^6 valves/g), which also had the highest SW index value. The nearshore areas had the lowest diatom concentrations, with site Y4 showing an almost complete absence of diatoms and the lowest SW index.

In January 2021, the diatom concentration peaked in the offshore areas, showing significant variation compared to the other zones. The highest values occurred at site W1 (2.64×10^6 valves/g) in the offshore area and the lowest concentrations occurred at the nearshore sites. The area with a low SW index expanded substantially in January compared to October, forming a roughly north-south distribution that roughly divides the study area into three parts. The SW index was relatively high in the estuarine areas, northern part of the central area, and offshore areas and relatively low in the nearshore areas, southern part of the central area, and Minjiang River estuary area.

Generally, low diatom concentrations were recorded in April 2021. The SW index exhibited relatively minor variations across the entire study area, with slightly lower values in the estuarine and nearshore regions than in the central and offshore areas.

3.1.2 *PCA of modern environmental variables*

PCA of all environmental variables, including SST, SSS, pH, redox potential, electrical conductivity, dissolved oxygen, total dissolved solids, turbidity, and sedimentary mean grain size, was performed to reduce the dimensionality of the dataset and determine the major environmental gradients (Abdi and Williams, 2010). The eigenvalues of the first two principal components (PC1 and PC2) were all greater than 1 and the cumulative proportion of these components was 72.4%, therefore, they were used to explain the main environmental variables.

The factor loading matrix expressed the loading (or degree of influence) of each variable on each principal component. Varimax rotation was applied to the factor-loading matrix and the coefficients of the principal components are shown in Fig. 3. PC1 was strongly related to SSS (52.2%) and PC2 was strongly related to SST (50.6%). Therefore, we concluded that SSS and SST have the greatest influence on the aquatic environment in the study area.

3.1.3 *Diatom species–environmental variables relationships*

The gradient length of the first axis in the DCA was 2.68 SD, indicating that the diatom data had a nonlinear unimodal distribution (Ter Braak et al., 1988). This implied that the optimal or highest concentration of diatoms occurred within a specific

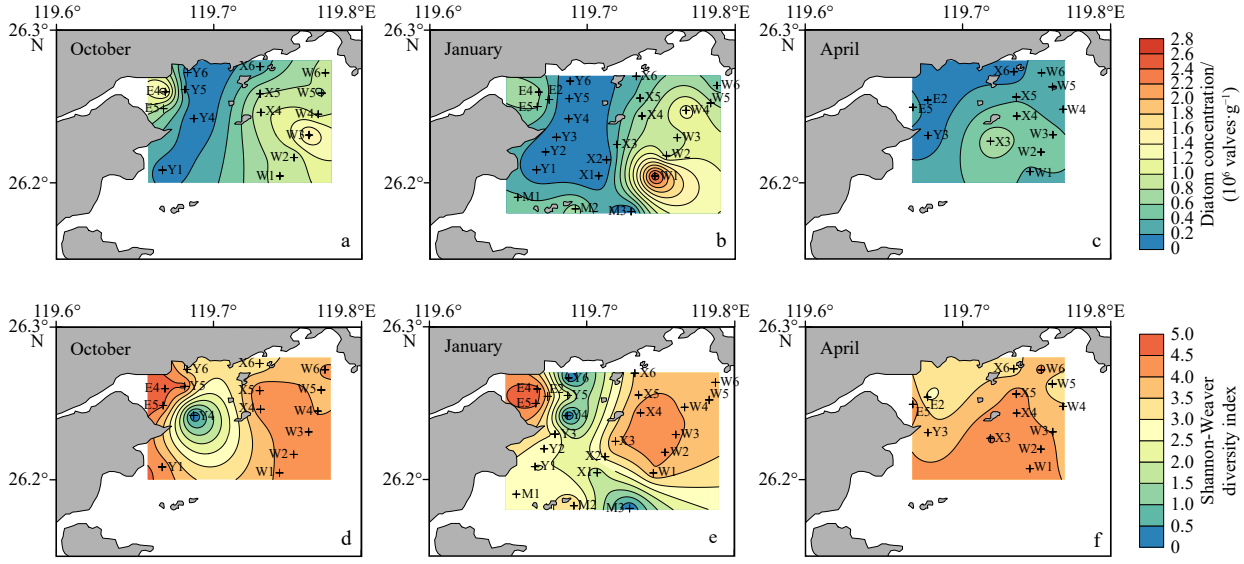

Fig. 2. Spatial distribution of diatom concentrations and the Shannon-Weaver diversity index of diatoms in surface sediment samples from the Lianjiang coastal area. a and d refer to October, b and e to January, c and f to April.

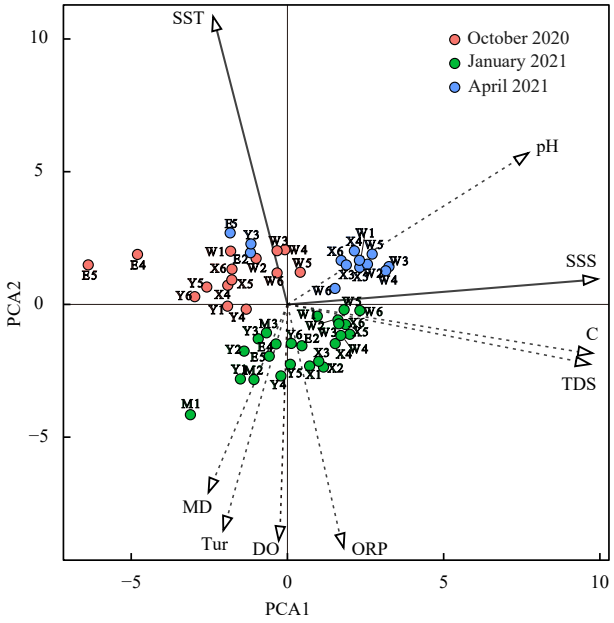

Fig. 3. Summary of the results of the Principal Correspondence Analysis (PCA) of the environmental variables: variable loadings (arrows) and sample scores (coloured symbols) on PC1 and PC2. The solid arrows represent the primary environmental factors that have the maximum load on PCA1 and PCA2, respectively, and the dashed arrows represent secondary impact factors. The angle between arrows indicates the correlation between individual environmental variables. SST: sea surface temperature; ORP: redox potential; C: conductivity; Tur: turbidity; DO: dissolved oxygen; TDS: total dissolved solids; SSS: sea surface salinity; MD: sediment mean grain size.

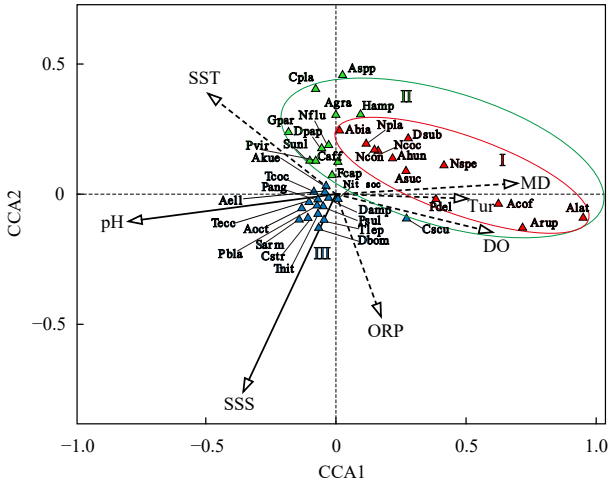

Fig. 4. Canonical correspondence analysis (CCA) biplot of environmental variables and diatoms species. See Table S2 for abbreviations. Red symbols: diatoms associated with coarse-grained sediments (Zone Ⅰ); green symbols: main freshwater diatom species (Zone Ⅱ); blue symbols: predominantly marine diatoms (Zone Ⅲ). SST: sea surface temperature; ORP: redox potential; Tur: turbidity; DO: dissolved oxygen; SSS: sea surface salinity; MD: sediment mean grain size.

range of habitat gradients. Therefore, the unimodal ordination technique of CCA was used to investigate the relationships between the environmental variables and diatom species from the surface samples. The Variance Inflation Factor (VIF) for each environmental variable was used to determine whether it independently affected the distribution of diatom combinations. The VIF results showed that the SSS, electrical conductivity, and total dissolved solids did not pass the test (VIF > 20). The strong correlation among these three factors indicates a large overlap in the provision of information on the aquatic environment (Blaine McCleskey et al., 2023). After excluding electrical conductivity and total dissolved solids, the remaining environmental variables (SST, SSS, pH, redox potential, dissolved oxygen, turbidity, and sedimentary mean grain size) passed the VIF and Monte Carlo permutations tests (999 unrestricted permutations, $p < 0.05$).

The CCA results showed that the pseudo-canonical correlations of CCA1 and CCA2 were 0.879 and 0.757, respectively, with the first two axes accounting for 74.67% of the total variances. This indicates that most of the constrained variance can be explained by the two axes.

The contributions of each factor to the CCA axis are shown in Fig. 4. The primary environmental factor influencing CCA1 was pH, which accounted for 79.8% of the total variance. The sedimentary mean grain size contributed 69.2% to CCA1, making it the second most influential factor. SSS had the highest contribution rate (75.4%) to CCA2. Consequently, pH and SSS were regarded as the most significant environmental factors affecting the distribution of diatom assemblages in the surface sediments of the study area, with the sedimentary mean grain size being the second most important factor.

The distribution of diatom species can be separated into three spatial zones based on the CCA findings of the diatom–environmental factors (Fig. 4). Zone Ⅰ is dominated by diatoms such as *Planothidium delicatulum, Achnanthes suchlandtii, Amphora coffeaeformis, Achnanthes laterostrata*, and *Navicula spectabilis*. These species were positively correlated with sedimentary mean grain size and turbidity and negatively correlated with pH and SSS. This indicates that they tend to accumulate in areas with coarse-grained sediments, high turbidity, low alkalinity, and high SSS. The nearshore and southern parts of the intertidal zone were the main areas of coarse-grained sediments. Freshwater diatoms transported by the Aojiang and Minjiang rivers enter this area and because of directional sorting, only a small portion of the smaller freshwater diatoms are retained in this area. The relationship between freshwater diatoms and coarse-grained sediments reflects the direct environmental effects on the deposition of marine microorganisms. Zone Ⅱ was characterised by *Aulacoseira granulata, Gomphonema parvulum, Cymbella affinis*, and *Fragilaria capucina*. Compared to Zone Ⅰ, these species were negatively correlated with SSS but were uncorrelated with the sedimentary mean grain size. Zone Ⅲ was characterised by marine diatom species that occur within the study region, including *Actinocyclus octonarius, Cyclotella striata, Diploneis bombus, Nitzschia sociabilis, Paralia sulcata, Surirella armoricana, Thalassionema nitzschioides, Thalassiosira eccentrica,* and *Tryblioptychus cocconeisformis.* They are concentrated at the centre of Fig. 4 in the positive direction of the SSS.

3.2 *Age model for sediment core HK3*

The calculated $^{210}Pb_{ex}$ activity varied from (54.3 ± 9.4) Bq/kg to (161.9 ± 11.45) Bq/kg in core HK3 (Fig. 5). Based on the characteristics of the calculated $^{210}Pb_{ex}$ activity, a CIC model was used to calculate the sedimentation rates of core HK3, which were determined to be 2.56 cm/a. These results are supported by Li et al. (2009) and Liu et al. (2009). The ^{210}Pb chronology indicated dates of AD 1884 at a depth of 95–96 cm and AD 2021 at a depth of 0–1 cm.

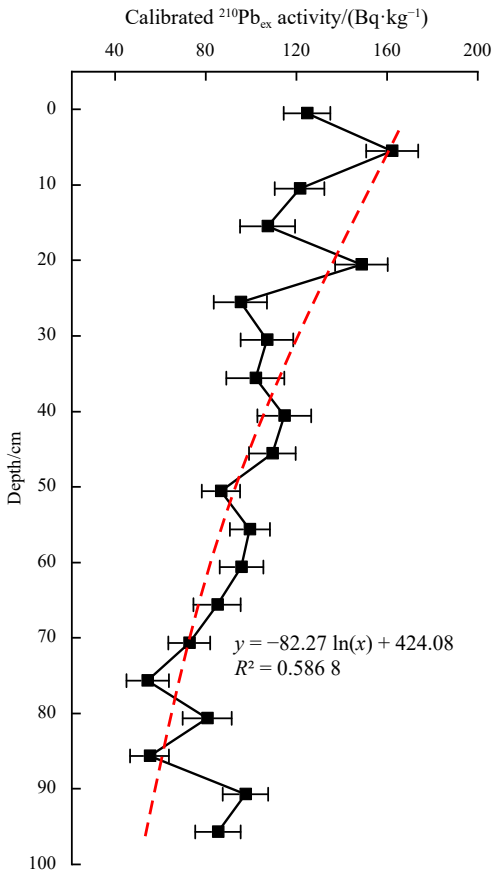

Fig. 5. Vertical profiles of $^{210}Pb_{ex}$ activity, clay content, and calculated $^{210}Pb_{ex}$ activity in core HK3. Error bars consider counting statistics uncertainties at 2σ.

3.3 *Development of diatom-based transfer functions*

The CCA results showed that pH and SSS were the primary environmental factors influencing diatom distribution, whereas the PCA results indicated that SSS was the most influential factor in the study area. Similarly, the relative explanatory power of SSS as a predictor of diatom assemblage composition can be estimated by calculating the ratio of the eigenvalue of the first constrained axis ($\lambda 1$) with SSS as a single explanatory variable with the first unconstrained axis ($\lambda 2$). The ratio $\lambda 1/\lambda 2$ is 2.468 (>1.0), indicating that SSS is the main determinant of diatom distribution in the training set (Ter Braak and Colin Prentice, 1988) (Table 1). Previous studies have also indicated that SSS is one of the most important factors controlling diatom distribution in estuarine environments (Hassan et al., 2007, 2009; Nwe et al., 2021; Sarker et al., 2020). Therefore, a diatom-based SSS transfer function was developed to reconstruct the past changes in coastal environments.

Table 1. Results of the $\lambda 1/\lambda 2$ test of each environmental variable

Variable	$\lambda 1$	$\lambda 2$	$\lambda 1/\lambda 2$
SSS	0.072	0.029	2.468
SST	0.025	0.085	0.292
pH	0.092	0.111	0.825
ORP	0.054	0.063	0.857
Tur	0.031	0.082	0.377
DO	0.038	0.091	0.415
MD	0.053	0.114	0.469

Note: SSS: sea surface salinity; SST: sea surface temperature; ORP: redox potential; Tur: turbidity; DO: dissolved oxygen; MD: sediment mean grain size.

Four numerical reconstruction methods were used to define the optimal diatom-based SSS transfer function (Table S3). The PLS method with 3 and 5 components resulted in a high R^2_{Jack} (0.32 and 0.36), along with lower $RMSEP_{Jack}$ (1.34 and 1.31) and maximum $bias_{Jack}$ (4.56 and 3.91) (Table S3). The WA-PLS method with 4 and 5 components also resulted in a high R^2_{Jack} (0.36 and 0.37), as well as low $RMSEP_{Jack}$ (1.29 and 1.29) and maximum $bias_{Jack}$ (3.02 and 3.11) (Table S3). Additionally, a plot of reconstructed SSS versus observed SSS showed a strong linear correlation, with randomly scattered residuals (Fig. 6). Hence, these four numerical reconstruction methods can be employed to obtain diatom-based SSS in the Lianjiang coastal area.

3.4 *Reliability of the diatom-based SSS reconstruction*

The dominant species in core HK3 were similar to those observed in surface sediment samples, including *Achnanthes suchlandtii, Actinocyclus octonarius, Amphora coffeaeformis, Aulacoseira granulata, Cocconeis scutellum, Cyclotella striata, Cymbella affinis, Gomphonema parvulum, Nitzschia sociabilis, Planothidium delicatulum, Parakia sulcata*, and *Thalassionema nitzschioides*. This suggests a continuity of environmental change from the past to the present in this area, which enables us to reconstruct paleoenvironmental conditions using the transfer function.

To determine the best model and test the reliability of the diatom-based SSS transfer function, the diatom data from core HK3 were used to quantitatively reconstruct SSS changes using the four models screened above and the reconstructed SSS were compared with modern SSS data. The results showed that the PLS method (Figs 7c and d) was superior to the WA-PLA method (Figs 7a and b) in terms of reconstruction, with a high correlation coefficient and more significant *p*-values than modern SSS data. In contrast, the PLS model with three components (Fig. 7c) had a higher correlation coefficient (0.517) and more significant *p*-value (0.001). Thus, the reconstructed SSS in core HK3 using the PLS model with three components was found to best match the actual SSS variations in the study area and was the most effective model for SSS reconstruction in this area.

The reconstructed SSS shows three low-SSS events, occurring in AD 2019, 2013, and 1999 (Fig. 8), coinciding with remarkably low diatom concentrations and SW index, accompanied by an increase in the relative abundance of freshwater diatoms (Figs 4 and 8; Zones Ⅰ and Ⅱ) and a decrease in the relative abundance of marine diatoms (Figs 4 and 8; Zone Ⅲ). Abrupt low SSS and diatom concentrations, as well as abrupt increases in freshwater diatoms to the marine environment, are probably related to typhoons and floods (Yang et al., 2023). In 2018, Super Typhoon Maria made direct landfall in Lianjiang County, with extraordinarily heavy rainfall of more than 200 mm (Liu et al., 2022). In 2013, Super Typhoon Soulik made landfall along the Huangqi Peninsula coast in Lianjiang County, bringing heavy rainfall to Fujian, and the Minjiang River caused excessive flooding. Additionally, the low SSS in 1999 corresponded to a catastrophic flood event in 1998, when a major flood occurred in the Minjiang River, with the maximum inflow at the Minjiang Estuary Power Station reaching 37 000 m^3/s, exceeding the historical maximum. These rapid, high-amplitude increases in freshwater inflows were likely to significantly reduce the SSS, and affect the abundance and structure of the phytoplankton communities in estuarine areas (Qiu et al., 2019; Yang et al., 2023).

In addition, three low-SSS events in AD 2019, 2013, and 1999

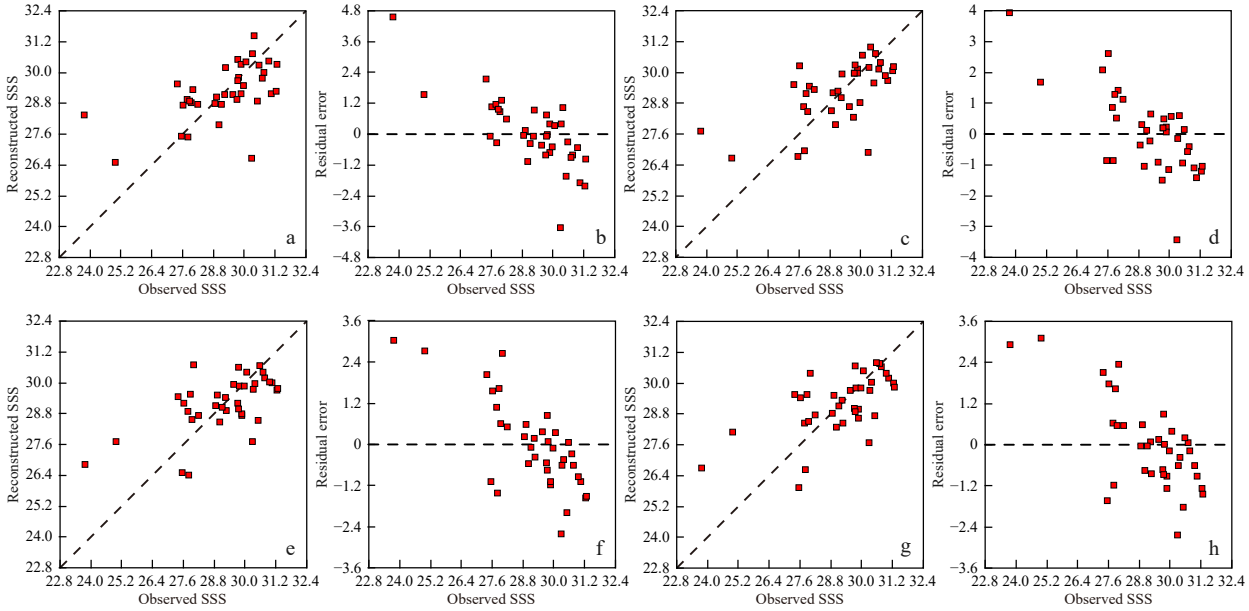

Fig. 6. Plots of observed versus predicted values and observed versus residual (predicted minus observed) values for four transfer function models derived for SSS. a and b: PLS with 3 components model; c and d: PLS with 5 components model; e and f: WA-PLS with 4 components model; g and h: WA-PLS with 5 components model.

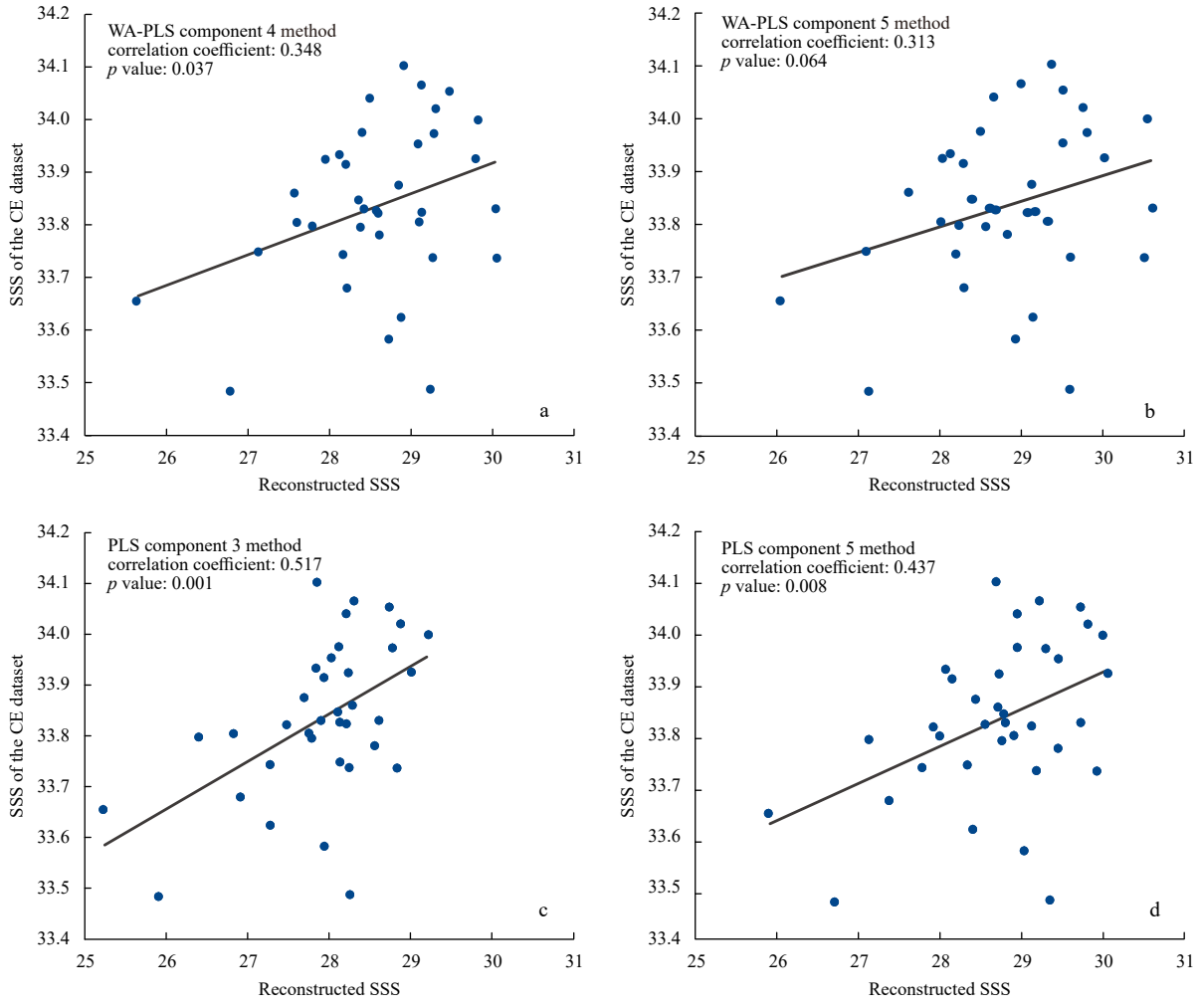

Fig. 7. Correlations between the diatom-based reconstructed SSS for core HK3 and the modern SSS data. a. WA-PLS with 4 components model. b. WA-PLS with 5 components model. c. PLS with 3 components model. d. PLS with 5 components model.

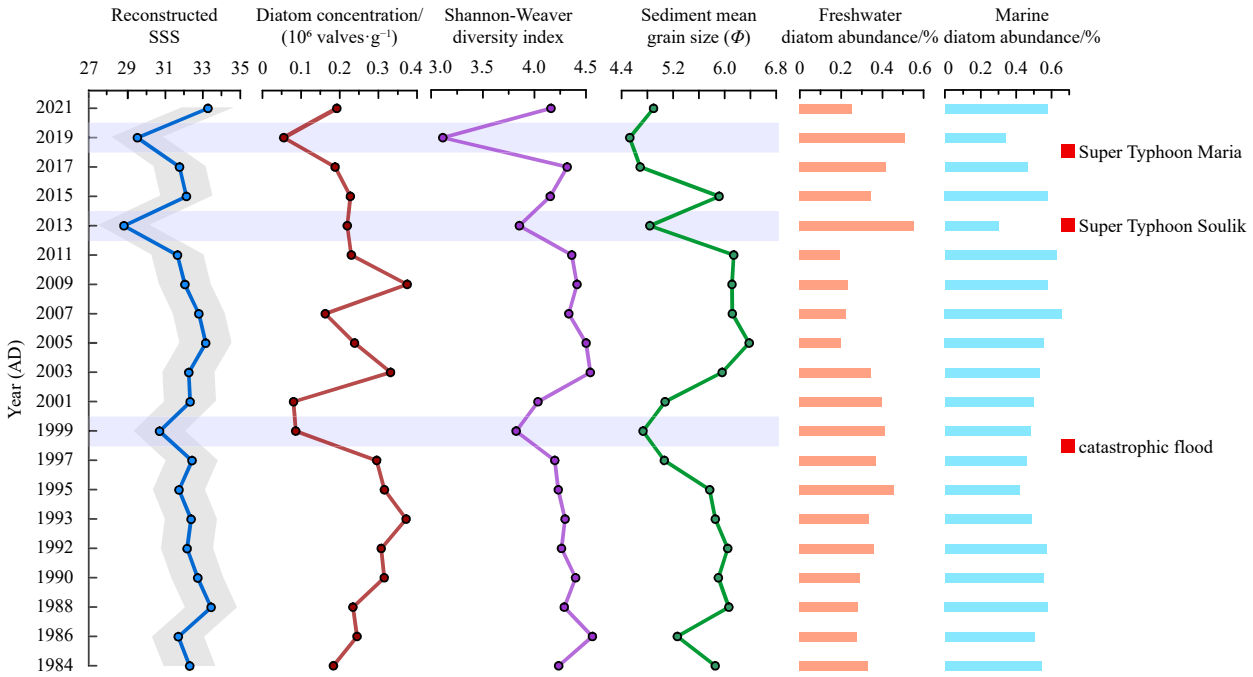

Fig. 8. Time series of reconstructed sea surface salinity (grey intervals are error values), diatom concentration, Shannon-Weaver diversity index, sediment mean grain size, and relative abundance of freshwater and marine diatom species in core HK3. Note that abrupt decreases in the SSS occurred in 2019, 2013, and 1999.

corresponded to coarser sedimentary grain sizes in core HK3 (Fig. 8). A study of the sedimentary processes revealed that the sediment discharged by rivers increases under the influence of typhoons and is then deposited in the estuary, accompanied by an expansion of the area of coarse-grained sediments (Yang et al., 2023). Rainfall triggered by a typhoon can cause a dramatic increase in river runoff to the sea, which is several tens of times higher than normal runoff (Zhao et al., 2008), whereas fine-grained suspended sediments remain in suspension and previously deposited fine-grained sediments within the coastal zone are resuspended and redistributed (Zang et al., 2018). This results in the coarsening of the sedimentary grain size and an increase in sand content (Lou et al., 2016).

The analysis of the correlation between the reconstructed SSS and the dominant diatom species showed a strong negative correlation (−0.858, $p < 0.01$) between salinity and the relative concentration of *Planothidium delicatulum*. *Planothidium delicatulum* is a freshwater diatom species commonly found in coastal areas with low salinity (Hartley et al., 1996). A study on the distribution of diatoms in the surface sediments of Qinzhou Bay and Zhenzhu Bay in Guangxi revealed that *Planothidium delicatulum* is mainly concentrated near the estuaries of the bays and is almost absent in the open sea, which can effectively indicate low sea surface salinity (Huang, 2017; Huang and Huang, 2016). *Planothidium delicatulum* is mainly found in the Aojiang and Minjiang river estuaries and rarely occurs offshore, also indicating its sensitivity to freshwater runoff. In addition, the relative concentrations of *Surirella armoricana* and *Cyclotella striata* showed a positive correlation with the reconstructed SSS, with a correlation of 0.6 ($p < 0.01$) and 0.51 ($p < 0.05$). *Surirella armoricana* and *Cyclotella striata* are marine benthic species that prefer brackish environments (Shang et al., 2023). Because the change in water salinity in estuarine coastal areas over a short period is closely related to the dilution effect of runoff injection, the variations in *Planothidium delicatulum, Surirella armoricana,* and *Cyclotella striata* are likely to be important indicators of river action intensity in estuarine coastal areas, indicating extreme events such as typhoons, rainstorms, and floods.

4 Conclusions

To quantify the relationship between coastal sediment diatoms and environmental variables in the Lianjiang River estuarine coastal areas and construct diatom-environment transfer functions, 52 surface sediment diatom samples and nine types of environmental factors were collected. The dominant diatom species in this region were *Actinocylus octonarius*, *Amphora coffeaeformis*, *Actinocyclus kuetzingii*, *Cyclotella striata*, *Paralia sulcata*, *Pleurosigma angulatum*, *Planothidium delicatulum*, *Surirella armoricana*. The diatom concentrations and SW index were relatively high in the estuary and offshore areas and lower in the nearshore areas.

The PCA results showed that the SSS and SST had the highest contribution rates to the PC1 and PC2 axes. CCA results indicated that pH and SSS were the most important environmental factors affecting the distribution of diatom assemblages in the surface sediments of the study area. The inferred SSS, based on PLS with 3 components model, best matched the actual SSS variation in the study area. This model was used to quantitatively reconstruct the SSS changes from 1984 to 2021 and the results were in good agreement with the measured SSS. In particular, the low SSS events in 1999, 2013, and 2019 were consistent with an increase in the relative concentration of freshwater diatoms and the coarsening of sediment grain size records, corresponding to two super-typhoon events and an extreme flood event in Lianjiang County. This transfer function is potentially useful for reconstructing past SSS in estuarine coastal regions with applications in future paleoceanographic studies.

Acknowledgements

We thank the editor and two anonymous reviewers for valuable comments to improve the manuscript.

References

Abdi H, Williams L J. 2010. Principal component analysis. WIREs Computational Statistics, 2(4): 433–459, doi: 10.1002/wics.101

Azhikodan G, Yokoyama K. 2015. Temporal and spatial variation of mixing and movement of suspended sediment in the Macrotidal Chikugo River Estuary. Journal of Coastal Research, 31(3): 680–689, doi: 10.2112/JCOASTRES-D-14-00097.1

Battarbee R W, Jones V J, Flower R J, et al. 2001. Diatoms. In: Smol J, Birks H, Last W, eds. Tracking Environmental Change Using Lake Sediments Volume 3: Terrestrial, Algal, and Siliceous Indicators. Dordrecht: Springer, 155–202

Benito G, Macklin M G, Zielhofer C, et al. 2015. Holocene flooding and climate change in the Mediterranean. CATENA, 130: 13–33, doi: 10.1016/j.catena.2014.11.014

Bennion H, Appleby P G, Phillips G L. 2001. Reconstructing nutrient histories in the Norfolk Broads, UK: implications for the role of diatom-total phosphorus transfer functions in shallow lake management. Journal of Paleolimnology, 26(2): 181–204, doi: 10.1023/A:1011137625746

Blaine McCleskey R, Cravotta III C A, Miller M P, et al. 2023. Salinity and total dissolved solids measurements for natural waters: An overview and a new salinity method based on specific conductance and water type. Applied Geochemistry, 154: 105684, doi: 10.1016/j.apgeochem.2023.105684

Chen Min, Li Yunhai, Qi Hongshuai, et al. 2019. The influence of season and Typhoon Morakot on the distribution of diatoms in surface sediments on the inner shelf of the East China Sea. Marine Micropaleontology, 146: 59–74, doi: 10.1016/j.marmicro.2019.01.003

Chen Xu, Liang Jia, Zeng Linghan, et al. 2022. Heterogeneity in diatom diversity response to decadal scale eutrophication in floodplain lakes of the middle Yangtze reaches. Journal of Environmental Management, 322: 116164, doi: 10.1016/j.jenvman.2022.116164

Chen Xu, McGowan S, Bu Zhaojun, et al. 2020b. Diatom-based water-table reconstruction in *Sphagnum* peatlands of northeastern China. Water Research, 174: 115648, doi: 10.1016/j.watres.2020.115648

Chen Min, Qi Hongshuai, Intasen W, et al. 2020a. Distributions of diatoms in surface sediments from the Chanthaburi coast, Gulf of Thailand, and correlations with environmental factors. Regional Studies in Marine Science, 34: 100991, doi: 10.1016/j.rsma.2019.100991

Chen Xiang, Zhou Weiqi, Pickett S T A, et al. 2016. Diatoms are better indicators of urban stream conditions: A case study in Beijing, China. Ecological Indicators, 60: 265–274, doi: 10.1016/j.ecolind.2015.06.039

De Sève M A. 1999. Transfer function between surface sediment diatom assemblages and sea-surface temperature and salinity of the Labrador Sea. Marine Micropaleontology, 36(4): 249–267, doi: 10.1016/S0377-8398(99)00005-5

Espinosa M A, Fayó R, Vélez-Agudelo C. 2022. Diatom-based paleoenvironmental reconstruction from the coast of Northern Patagonia, Argentina. Journal of South American Earth Sciences, 116: 103874, doi: 10.1016/j.jsames.2022.103874

Fan Jiayu, Jian Xing, Shang Fei, et al. 2021. Underestimated heavy metal pollution of the Minjiang River, SE China: Evidence from spatial and seasonal monitoring of suspended-load sediments. Science of the Total Environment, 760: 142586, doi: 10.1016/j.scitotenv.2020.142586

Fayó R, Espinosa M A, Vélez-Agudelo C A, et al. 2018. Diatom-based reconstruction of Holocene hydrological changes along the Colorado River floodplain (northern Patagonia, Argentina). Journal of Paleolimnology, 60(3): 427–443, doi: 10.1007/s10933-018-0031-2

Gomes D F, Albuquerque A L S, Torgan L C, et al. 2014. Assessment of a diatom-based transfer function for the reconstruction of lake-level changes in Boqueirão Lake, Brazilian Nordeste. Palaeogeography, Palaeoclimatology, Palaeoecology, 415: 105–116, doi: 10.1016/j.palaeo.2014.07.009

Gregersen R, Howarth J D, Atalah J, et al. 2023. Paleo-diatom records reveal ecological change not detected using traditional measures of lake eutrophication. Science of the Total Environment, 867: 161414, doi: 10.1016/j.scitotenv.2023.161414

Guo Yujie, Qian Shuben. 2003. Flora algarum marinarum sinicarum (in Chinese), Volume 5, Diatom Phylum, Book 1, Central Outline. Beijing: Science Press, 1–493

Håkansson H. 1984. The recent diatom succession of Lake Havgårdssjön, South Sweden. In: Proceedings of the Seventh International Diatom Symposium. Philadelphia: Otto Koeltz, 411–429

Hartley B, Barber H G, Carter J R, et al. 1996. An Atlas of British Diatoms. Bristol: Biopress Ltd, 1–601

Hassan G S, Espinosa M A, Isla F I. 2007. Dead diatom assemblages in surface sediments from a low impacted estuary: the Quequén Salado river, Argentina. Hydrobiologia, 579(1): 257–270, doi: 10.1007/s10750-006-0407-6

Hassan G S, Espinosa M A, Isla F I. 2009. Diatom-based inference model for paleosalinity reconstructions in estuaries along the northeastern coast of Argentina. Palaeogeography, Palaeoclimatology, Palaeoecology, 275(1–4): 77–91, doi: 10.1016/j.palaeo.2009.02.020

Horton B P, Corbett R, Culver S J, et al. 2006. Modern saltmarsh diatom distributions of the Outer Banks, North Carolina, and the development of a transfer function for high resolution reconstructions of sea level. Estuarine, Coastal and Shelf Science, 69(3–4): 381–394, doi: 10.1016/j.ecss.2006.05.007

Huang Yue. 2017. Distribution of the surface sediment diatoms in the outer bay of Qinzhou bay of Guangxi. Marine Sciences (in Chinese), 41(1): 96–103, doi: 10.11759/hykx20150927001

Huang Yue, Huang Yuanhui. 2016. Characterastics of surface sediments diatom distribution in Zhenzhu Bay of Guangxi. Advances in Marine Science (in Chinese), 34(3): 411–420, doi: 10.3969/j.issn.1671-6647.0000.00.011

Huh Chih-An, Su Chih-Chieh. 1999. Sedimentation dynamics in the East China Sea elucidated from ^{210}Pb, ^{137}Cs and ^{239,240}Pu. Marine Geology, 160(1-2): 183–196, doi: 10.1016/S0025-3227(99)00020-1

Hustedt F. 1985. The Pennate Diatoms. Koenigstein: Koeltz Scientific Books, 1–918

Jiang Yamei, Saito Y, Ta T K O, et al. 2020. Spatial and seasonal variability in grain size, magnetic susceptibility, and organic elemental geochemistry of channel-bed sediments from the Mekong Delta, Vietnam: Implications for hydro-sedimentary dynamic processes. Marine Geology, 420: 106089, doi: 10.1016/j.margeo.2019.106089

Jiang Hui, Zheng Yulong, Ran Lihua, et al. 2004. Diatoms from the surface sediments of the South China Sea and their relationships to modern hydrography. Marine Micropaleontology, 53(3-4): 279–292, doi: 10.1016/j.marmicro.2004.06.005

Jin Dexiang, Cheng Zhaodi, Lin Junmin, et al. 1982. Chinese marine benthic diatoms (Volume 1) (in Chinese). Beijing: China Ocean Press, 17–236

Jousé A P, Kozlova O G, Muhina V V. 1971. Distribution of diatoms in the surface layer of sediment from the Pacific Ocean. In: Funnell B M, Riedel W R, eds. The Micropalaeontology of Oceans. London: Cambridge University Press, 263–269

Juggins S. 2007. C2 Version 1.5 User guide. Software for ecological and palaeoecological data analysis and visualisation. Newcastle upon Tyne: Newcastle University, 1–73

Klami A, Virtanen S, Kaski S. 2013. Bayesian Canonical correlation analysis. The Journal of Machine Learning Research, 14(1): 965–1003

Krammer K, Lange-Bertalot H. 1986. Bacillariophyceae 1. Teil: Naviculaceae. In: Ettl H, Gerloff J, Heynig H, et al, eds. Süsswasserflora von Mitteleuropa, Band 2/1. New York: Gustav Fisher Verlag, 1–876

Krammer K, Lange-Bertalot H. 1988. Bacillariophyceae 2. Teil: Bacillariaceae, epithemiaceae, surirellaceae. In: Ettl H, Gerloff J, Heynig H, Mollenhauer D, eds. Susswasserflora von Mitteleuropa, Band 2/2. Jena: Gustav Fisher Verlag

Krammer K, Lange-Bertalot H. 1991a. Bacillariophyceae 3. Teil:

Centrales, fragilariaceae, eunotiaceae. In: Ettl H, Gerloff J, Heynig H, Mollenhauer D, eds. Süsswasserflora von Mitteleuropa 2/3. Jena: Gustav Fisher Verlag, 1–576

Krammer K, Lange-Bertalot H. 1991b. Bacillariophyceae 4. Teil: Achnanthaceae, kritische ergänzungen zu navicula (Lineolatae) und gomphonema, gesamtliteraturverzeichnis Teil 1-4. In: Ettl H, Gerloff J, Heynig H, Mollenhauer D, eds. Süsswasserflora von Mitteleuropa 2/4. Jena: Gustav Fischer Verlag.

López-Belzunce M, Blázquez A M, Carmona P, et al. 2020. Multi proxy analysis for reconstructing the late Holocene evolution of a Mediterranean Coastal Lagoon: Environmental variables within foraminiferal assemblages. CATENA, 187: 104333, doi: 10.1016/j.catena.2019.104333

Lei Jiajun, Yang Liyang, Zhu Zhuoyi. 2021. Testing the effects of coastal culture on particulate organic matter using absorption and fluorescence spectroscopy. Journal of Cleaner Production, 325: 129203, doi: 10.1016/j.jclepro.2021.129203

Li Dongmei, Liu Guangshan, Li Chao, et al. 2009. Radionuclide distribution in sediments and sedimentary rates in seas surrounding Xiamen. Journal of Oceanography in Taiwan Strait (in Chinese), 28(3): 336–342

Li Dongling, Sha Longbin, Li Jialin, et al. 2017. Summer sea-surface temperatures and climatic events in Vaigat Strait, West Greenland, during the Last 5000 Years. Sustainability, 9(5): 704, doi: 10.3390/su9050704

Lin Xiaohong, Yin Siyu, Wu Wei, et al. 2020. Genetic diagnosis for heavy typhoon rainfall attenuated by Fujian landfall. Tropical Cyclone Research and Review, 9(3): 178–184, doi: 10.1016/j.tcrr.2020.08.001

Lionard M, Muylaert K, Hanoutti A, et al. 2008. Inter-annual variability in phytoplankton summer blooms in the freshwater tidal reaches of the Schelde estuary (Belgium). Estuarine, Coastal and Shelf Science, 79(4): 694–700, doi: 10.1016/j.ecss.2008.06.013

Liu Shenfa, Shi Xuefa, Liu Yanguang, et al. 2009. Sedimentation rate of mud area in the East China Sea inner continental shelf. Marine Geology & Quaternary Geology (in Chinese), 29(6): 1–7, doi: 10.3724/SP.J.1140.2009.06001

Liu Jingli, Zhang Han, Zhong Rui, et al. 2022. Impacts of wave feedbacks and planetary boundary layer parameterization schemes on air-sea coupled simulations: A case study for Typhoon Maria in 2018. Atmospheric Research, 278: 106344, doi: 10.1016/j.atmosres.2022.106344

Lou Sha, Huang Wenrui, Liu Shuguang, et al. 2016. Hurricane impacts on turbidity and sediment in the Rookery Bay National Estuarine Research Reserve, Florida, USA. International Journal of Sediment Research, 31(4): 330–340, doi: 10.1016/j.ijsrc.2016.06.006

Mendes S, Fernández-Gómez M J, Resende P, et al. 2009. Spatio-temporal structure of diatom assemblages in a temperate estuary. A STATICO analysis. Estuarine, Coastal and Shelf Science, 84(4): 637–644, doi: 10.1016/j.ecss.2009.08.003

Nakanishi R, Ashi J, Miyairi Y, et al. 2022. Holocene coastal evolution, past tsunamis, and extreme wave event reconstructions using sediment cores obtained from the central coast of Hidaka, Hokkaido, Japan. Marine Geology, 443: 106663, doi: 10.1016/j.margeo.2021.106663

Nwe L W, Azhikodan G, Yokoyama K, et al. 2021. Spatio-temporal distribution of diatoms and dinoflagellates in the macrotidal Tanintharyi River estuary, Myanmar. Regional Studies in Marine Science, 42: 101634, doi: 10.1016/j.rsma.2021.101634

Peng Tong, Zhu Zhuoyi, Du Jinzhou, et al. 2021. Effects of nutrient-rich submarine groundwater discharge on marine aquaculture: A case in Lianjiang, East China Sea. Science of The Total Environment, 786: 147388, doi: 10.1016/j.scitotenv.2021.147388

Prelle L R, Graiff A, Gründling-Pfaff S, et al. 2019. Photosynthesis and respiration of baltic sea benthic diatoms to changing environmental conditions and growth responses of selected species as affected by an adjacent peatland (Hütelmoor). Frontiers in Microbiology, 10: 1500, doi: 10.3389/fmicb.2019.01500

Qiu Dajun, Zhong Yu, Chen Yongqiang, et al. 2019. Short-term phytoplankton dynamics during typhoon season in and near the Pearl River Estuary, South China Sea. Journal of Geophysical Research: Biogeosciences, 124(2): 274–292, doi: 10.1029/2018JG004672

Ran Lihua, Jiang Hui. 2005. Distributions of the surface sediment diatoms from the south China sea and their palaeoceanographic significance. Acta Micropalaeontologica Sinica, 22(1): 97–106

Rovira L, Trobajo R, Ibáñez C. 2012. The use of diatom assemblages as ecological indicators in highly stratified estuaries and evaluation of existing diatom indices. Marine Pollution Bulletin, 64(3): 500–511, doi: 10.1016/j.marpolbul.2012.01.005

Saifullah A S M, Kamal A H M, Idris M H, et al. 2019. Community composition and diversity of phytoplankton in relation to environmental variables and seasonality in a tropical mangrove estuary. Regional Studies in Marine Science, 32: 100826, doi: 10.1016/j.rsma.2019.100826

Sanchez-Cabeza J A, Ruiz-Fernández A C. 2012. ^{210}Pb sediment radiochronology: An integrated formulation and classification of dating models. Geochimica et Cosmochimica Acta, 82: 183–200, doi: 10.1016/j.gca.2010.12.024

Sarker S, Yadav A K, Shahadat Hossain M, et al. 2020. The drivers of diatom in subtropical coastal waters: A Bayesian modelling approach. Journal of Sea Research, 163: 101915, doi: 10.1016/j.seares.2020.101915

Sha Longbin, Jiang Hui, Liu Yanguang, et al. 2015. Palaeo-sea-ice changes on the North Icelandic shelf during the last millennium: Evidence from diatom records. Science China Earth Sciences, 58(6): 962–970, doi: 10.1007/s11430-015-5061-2

Shang Zhiwen, Li Jianfen, Freund H, et al. 2023. Quantitative relationship between surface sedimentary diatoms and water depth in North-Central Bohai Bay, China. China Geology, 6(1): 61–69, doi: 10.31035/cg2022040

Shannon C E, Weaver W. 1949. The Mathematical Theory of Communication. Urbana: The University of Illinois Press, 1–117

Sun Xueshi, Fan Dejiang, Liao Huijie, et al. 2020. Variation in sedimentary ^{210}Pb over the last 60 years in the Yangtze River Estuary: New insight to the sedimentary processes. Marine Geology, 427: 106240, doi: 10.1016/j.margeo.2020.106240

Sun Xueshi, Fan Dejiang, Tian Yuan, et al. 2017. Normalization of excess ^{210}Pb with grain size in the sediment cores from the Yangtze River Estuary and adjacent areas: Implications for sedimentary processes. The Holocene, 28(4): 545–557, doi: 10.1177/0959683617735591

Szczerba A, Rzodkiewicz M, Tylmann W. 2023. Modern diatom assemblages and their association with meteorological conditions in two lakes in northeastern Poland. Ecological Indicators, 147: 110028, doi: 10.1016/j.ecolind.2023.110028

Ter Braak C J F, Colin Prentice I. 1988. A theory of gradient analysis. Advances in Ecological Research, 18: 271–317, doi: 10.1016/S0065-2504(08)60183-X

Ter Braak C J F, Smilauer P. 2012. Canoco Reference Manual and User's Guide: Software for Ordination, Version 5.0. Ithaca: Microcomputer Power.

Triantaphyllou M V, Ziveri P, Gogou A, et al. 2009. Late Glacial–Holocene climate variability at the south-eastern margin of the Aegean Sea. Marine Geology, 266(1–4): 182–197, doi: 10.1016/j.margeo.2009.08.005

Wang Rong, Dearing J A, Langdon P G, et al. 2012. Flickering gives early warning signals of a critical transition to a eutrophic lake state. Nature, 492(7429): 419–422, doi: 10.1038/nature11655

Wang Zhanghua, Jones B G, Chen Ting, et al. 2013. A raised OIS 3 sea level recorded in coastal sediments, southern Changjiang delta plain, China. Quaternary Research, 79(3): 424–438, doi: 10.1016/j.yqres.2013.03.002

Wang Qian, Yang Xiangdong, John Anderson N, et al. 2014. Diatom response to climate forcing of a deep, alpine lake (Lugu Hu, Yunnan, SW China) during the Last Glacial Maximum and its implications for understanding regional monsoon variability. Quaternary Science Reviews, 86: 1–12, doi: 10.1016/j.quascirev.2013.12.024

Xu Zhimeng, Li Yifan, Lu Yanhong, et al. 2020. Impacts of the Zhe-

Min Coastal Current on the biogeographic pattern of microbial eukaryotic communities. Progress in Oceanography, 183: 102309, doi: 10.1016/j.pocean.2020.102309

Yang Liyang, Chen Yu, Lei Jiajun, et al. 2022. Effects of coastal aquaculture on sediment organic matter: Assessed with multiple spectral and isotopic indices. Water Research, 223: 118951, doi: 10.1016/j.watres.2022.118951

Yang Xiangdong, John Anderson N, Dong Xuhui, et al. 2008. Surface sediment diatom assemblages and epilimnetic total phosphorus in large, shallow lakes of the Yangtze floodplain: their relationships and implications for assessing long-term eutrophication. Freshwater Biology, 53(7): 1273–1290, doi: 10.1111/j.1365-2427.2007.01921.x

Yang Shangshang, Li Yunhai, Lin Yunpeng, et al. 2023. Evolution of sedimentary dynamic process/pattern in the Quanzhou Bay under impact of Typhoon Matmo (2014). Regional Studies in Marine Science, 62: 102974, doi: 10.1016/j.rsma.2023.102974

Yu Fengling, Li Nannan, Tian Ganghua, et al. 2023a. A re-evaluation of Holocene relative sea-level change along the Fujian coast, southeastern China. Palaeogeography, Palaeoclimatology, Palaeoecology, 622: 111577,doi: 10.1016/j.palaeo.2023.111577

Yu Siwei, Wang Junbo, Rühland K M, et al. 2023b. Spatial distribution of surface-sediment diatom assemblages from 45 Tibetan Plateau lakes and the development of a salinity transfer function. Ecological Indicators, 155: 110952, doi: 10.1016/j.ecolind.2023.110952

Zang Zhengchen, George Xue Z, Bao Shaowu, et al. 2018. Numerical study of sediment dynamics during hurricane Gustav. Ocean Modelling, 126: 29–42, doi: 10.1016/j.ocemod.2018.04.002

Zhang Rijun. 2014. Construction of digital Aojiang watershed. Applied Mechanics and Materials, 687–691: 2157–2160, doi: 10.4028/www.scientific.net/AMM.687-691.2157

Zhao Hui, Tang Danling, Wang Yuqing. 2008. Comparison of phytoplankton blooms triggered by two typhoons with different intensities and translation speeds in the South China Sea. Marine Ecology Progress Series, 365: 57–65, doi: 10.3354/meps07488

Zhou Min, Fang Futao, Zeng Cong, et al. 2022. Community competition is the microorganism feedback to sedimentary carbon degradation process in aquaculture tidal flats. Frontiers in Marine Science, 9: 880120., doi: 10.3389/fmars.2022.880120

Zong Yongqiang, Horton B P. 1999. Diatom-based tidal-level transfer functions as an aid in reconstructing Quaternary history of sea-level movements in the UK. Journal of Quaternary Science, 14(2): 153–167, doi: 10.1002/(SICI)1099-1417(199903)14:2<153::AID-JQS425>3.0.CO;2-6

Supplementary information:

Table S1. Environmental variables in surface sampling sites.

Table S2. Full names and abbreviations of the main diatom species in the Lianjiang coastal area.

Table S3. Results of method testing for transfer function. Maximum bias (Max $\text{Bias}_{\text{Jack}}$), coefficient of determination between observed and predicted values R^2_{Jack}, and root mean squared error of prediction, based on the leave-one-out jack-knifing ($\text{RMSEP}_{\text{Jack}}$) for the reconstructed SSS in seven reconstruction procedures. WA: weighted averaging regression and calibration, calibration, WA(tol): weighted averaging with tolerance downweighting, PLS: partial least squares, WA-PLS: weighted averaging with partial least squares, IKM: Imbrie and Kipp Model. Both the inverse and classical deshrinking regressions were used in the WA and WA(tol) reconstruction procedures. The tests showed that PLS with three and five components and WA-PLS with four and five components were the most reliable (values in bold).

Figure S1. Dominant and typical diatoms on the Lianjiang coast.

The supplementary information is available online at https:// doi.org/10.1007/s13131-024-2292-0 and http://www.aosocean.com/. The supplementary information is published as submitted, without typesetting or editing. The responsibility for scientific accuracy and content remains entirely with the authors.